Magnetic chitosan physicochemical properties to improve treated water quality

M.C. Estephany Santiago Siliceo[a], Dr Sergio Perez Sicairos[b], Dra Georgina Pina Luis[c], Dr Oscar Perez Landeros[d], Dr Navor Rosas González[e], Dr Benjamín Valdez Salas[f], Dra Mercedes Teresita Oropeza Guzmán[*].

[a] Tecnológico Nacional de México/Instituto Tecnológico de Tijuana, Centro de Graduados de Investigación en Química, Blvd. Alberto Limón Padilla s/n, Col. Otay, Tijuana, B.C. 22500 MX, estephanysantiago@gmail.com, Tijuana, Baja California, México.

[b] Tecnológico Nacional de México/Instituto Tecnológico de Tijuana, Centro de Graduados de Investigación en Química, Blvd. Alberto Limón Padilla s/n, Col. Otay, Tijuana, B.C. 22500 MX, sperez@tectijuana.mx, Tijuana, Baja California, México.

[c] Tecnológico Nacional de México/Instituto Tecnológico de Tijuana, Centro de Graduados de Investigación en Química, Blvd. Alberto Limón Padilla s/n, Col. Otay, Tijuana, B.C. 22500 MX, gpinaluis@yahoo.com, Tijuana, Baja California, México.

[d] Universidad Autónoma de Baja California, Campus Mexicali, Instituto de Ingeniería, Mexicali, B.C. MX, oscar.manuel.perez.landeros@uabc.edu.mx, Mexicali, Baja California, México

[e] Universidad Autónoma de Baja California, Campus Mexicali, Instituto de Ingeniería, Mexicali, B.C. MX, navor14@gmail.com, Mexicali, Baja California, México

[f] Universidad Autónoma de Baja California, Campus Mexicali, Instituto de Ingeniería, Mexicali, B.C. MX, benval@uabc.edu.mx, Mexicali, Baja California, México

[*] Tecnológico Nacional de México/Instituto Tecnológico de Tijuana, Posgrado en Ciencias de la Ingeniería, Blvd. Alberto Limón Padilla s/n, Col. Otay, Tijuana, B.C. 22500 MX. Oropeza1@yahoo.com, Tijuana, Baja California, México

Resumen

Las tecnologías de tratamiento de agua, como la ósmosis inversa, la precipitación química, el intercambio de iones y la eliminación electroquímica, se utilizan generalmente para mejorar la calidad y la estética del agua (como la alcalinidad y la dureza). Sin embargo, estos procesos a menudo requieren un ajuste posterior al tratamiento que los hace onerosos.

En este artículo mostramos nanopartículas magnéticas de óxido de hierro y su modificación química con quitosano por el método de coprecipitación con alto potencial para ser utilizadas en la mejora de la calidad del agua de reúso. Se sintetizaron cinco tipos diferentes de quitosano magnético variando la cantidad de quitosano añadida a las nanopartículas antes de la nucleación de la magnetita. Todos los quitosanos magnéticos fueron estudiados y comparados por DLS y Potencial Zeta para elegir el material más prometedor para tratamientos de agua.

Los materiales magnéticos fueron caracterizados previamente a su uso mediante estudios FT-IR, SEM/STEM, Potencial Zeta, DLS y TGA, comprobando la unión entre magnetita y el biopolímero.

Se realizaron estudios de estos materiales magnéticos en agua de reúso, de la planta de tratamiento de aguas residuales "La Morita" (Tijuana, B. C., México), para comprobar su efectividad en la remoción de alcalinidad y dureza. Descubrimos que ambos materiales magnéticos demostraron ser efectivos para atrapar y eliminar carbonatos del agua recuperada. Al mismo tiempo, tenemos la posibilidad de recuperarlos para usos posteriores y reducir el costo de operación. Con todas estas características podemos clasificar los materiales preparados como nano ablandadores sustentables.

Palabras clave: Nanopartículas magnéticas de óxido de hierro, Nano ablandadores magnéticos, Quitosano magnético, Tratamiento de aguas, Tratamiento de aguas de reúso.

Abstract

Water treatment technologies such as reverse osmosis, chemical precipitation, ion exchange, and electrochemical removal, are generally used to improve water quality and aesthetics (such alkalinity and hardness). However, this processes often requires a post treatment adjustment making them onerous.

In this paper we show iron-oxide magnetic nanoparticles and its chemical modification with chitosan by co-precipitation method with high potential to be used on reclaimed water quality improvement. Five different types of magnetic chitosan were synthetized varying the amount of chitosan added to the nanoparticles, previous the nucleation of the magnetite. All the magnetic chitosan were studied and compared by DLS and Zeta potential to choose the most promising material for water treatment.

The magnetic materials were characterized previous their use by FT-IR, SEM/STEM, Zeta Potential, DLS, and TGA studies, proving the binding between magnetite and the biopolymer.

Studies of the magnetic materials on reclaimed water, from the wastewater treatment plant "La Morita" (Tijuana, B.C., México), were carried out to prove their effectiveness to remove alkalinity and hardness. We found out that both magnetic materials proved to be effective for trap and remove carbonates from reclaimed water. At the same time, we have the possibility of recovering them to further uses and reduce the operation cost. With all these characteristics we can classify the prepared materials as sustainable nano softeners.

***Keywords**: Iron-oxide magnetic nanoparticles, Magnetic chitosan, Magnetic Nano-softeners, Reclaim water treatment, Water treatment*

1. INTRODUCTION

Present-day, it exists an increasing concern for the development of wastewater treatment technologies and reclaimed water reuse, where nanomaterials hierarchically-structured metal oxides have gained importance in their use in water treatment, one of these nanomaterials are the iron-oxide magnetic nanoparticles (MNP).[1] MNP have been on the spotlight due to their unique properties, which include extremely small size, high surface area/volume ratio, surface adaptability, biocompatibility and sterling magnetic properties.[2,3] The super paramagnetic properties of the magnetite make this material excellent for separation

processes with exertion of a magnetic field that selectively collect them. This characteristic makes them stand out over other nanomaterials used in water treatment, avoiding an additional separation step to remove such nanomaterials from solution. The application of MNP in water treatment is based on chemical or physical adsorption, therefore, not only organic substances can be removed, but also metal ions.[4]

One inconvenience of this material can be their fast agglomeration, but this can be easily fixed modifying the material using a coating. Various materials have been applied as coatings for MNP including organic nonpolymeric materials, polymeric materials, and inorganic molecules.[5] The coating principle can be based on covalent attachment, van der Waals interaction, and electrostatic interactions. The surface modification can not only alter the surface functional groups of MNP, but also improve the stability of nanoparticles against agglomeration.[4]

Despite the fact that most studies have focused on the development of the coating of MNP with small organic molecules and surfactants,[6–8] recently, functionalized MPN with polymers have being incorporated.[9] This fact highlight the advantages that polymers have coated the surface of MNP and increased repulsive forces in order to balance the forces of magnetic attraction and Van der Waals acting on the MNP. One biopolymer that has attracted great attention for its large potential applications in pharmaceuticals,[10,11] cosmetics,[12] biomedical/ biotechnological,[13,14] as well as food,[15] textile industry,[16] and water treatment,[17,18] is chitosan. This particular biopolymer has emerged as a new class of highly material with sophisticated functions due to their versatile biological activity, great biocompatibility, and complete biodegradability in combination with low toxicity.

Previous works prove the effectiveness of the MCH to remove heavy metal ions from water being able to remove Pb^{2+}, Cu^{2+}, and Cd^{2+}, because the inactive chitosan on the surface of the magnetic nanoparticles is coordinated with them.[1,4] In this work magnetic chitosan (MCH) nanocomposites have been synthesized and used to treat reclaim water to remove metal ions such as Ca^{2+} and Mg^{2+} due to its expecting excellent adsorption capacities.

MCH is a promising material for industrial scale wastewater treatment, due to their low cost, strong adsorption capacity, easy separation, and enhanced stability.

2. CONTENT

2.1 Materials and methods

Superparamagnetic iron-oxide nanoparticles (MNP) were synthesized via chemical co-precipitation as previously reported,[19] the methodology was inspired in the methodology reported by Liu et al[20] with some modifications.

The different Magnetic Chitosan (MCH) were also prepared by co-precipitation in one step as we reported[19] but changing the amount of modifier (CH): 100 mg, 200 mg (in powder as purchased, and in 1% acetic acid solution), and 1000 mg (in powder as purchased) to obtain: MCH-100, MCH-200, and, MCH-1000, by adding CH in powder; and MCH-100S and MCH-200S, by adding CH in 1% of acetic acid.

DLS and Zeta Potential and pH measurements were performed in an Anton Paar (Litesizer 500) to analyze the size of all nanoparticles and its dependence with the pH and their physicochemical performance, on a scale from 2 to 12. The pH was adjusted with 0.1 M HCl to pH = 2 and 0.1 M NaOH to pH 12.

Naked Magnetic nanoparticles (MNP) and the chosen MCH to perform water treatment were first characterized using abroad of techniques: (i) Fourier transform infrared spectroscopy (FT-IR) in powder was performed using a Shimadzu FT-IR (IRSpirit) ATR mode, to compare the functional groups on each material and validate the correct modification of the magnetite. (ii) Thermogravimetric analysis (TGA) using a Perkin Elmer equipment (TGA 4000) to examine the thermal decomposition in an inert atmosphere of argon (10 °C min^{-1}). The samples were heated from a temperature of 30 °C to 800 °C. The results were compared to evaluate the modification of the magnetic material. (iii) The surface areas of MNP and MCH were estimated by Brunauer-Emmett-Teller method (BET) in a Quantachrome Instruments, model autosorb iQ operated with the software Quantachrome AsiQwin. (iv) SEM for the MNP and STEM image for MCH were performed using a dual-beam focused ion beam/field emission scanning transmission electron microscope (Tescan Lyra 3GM). SEM and STEM micrographs were recorded with an accelerating voltage of 10 and 20 kV, respectively.

The Reclaim Water (RW) samples for this work were obtained from the wastewater treatment plant "La Morita" located in the city of Tijuana in the state of Baja California, México, this samples were treated with MNP and MCH to analyze the improvement of the water quality in terms of alkalinity and hardness removal. This study was performed at pH 7, 8, and 9. The methodology of this analysis is followed as reported in a previous work.[19]

2.2 Results and discussions

Naked magnetic nanoparticles (MNP) along with five different types of magnetite modified with chitosan (magnetic chitosan) were synthesized. These magnetic chitosan were obtained by adding different dosage (100, 200 and 1000 mg) and state of aggregation (powder or solution) of the biopolymer in the formation of the magnetite. Figure 1a shows the comparison of the hydrodynamic diameter and its dependence with the pH for MNP and the different magnetic chitosan. For MCH-100S it can be seen that the nanoparticles have more agglomeration from pH 3 to 6 and then from 8 to 12, and for MCH-200S its notable that adding more CH in acetic acid solution modifies the molecule that now present lower agglomerations at lower

pH values and increase its size along with the pH scale. Both MCHs have their biggest sizes close to their isoelectric point (IEP). We also can observe that adding more CH powder to the magnetic core gradually increase their size at pHs lower than 6 which is due to the gained stable aggregation and this stability can be seen on the Figure 1b, where all the MCHs have a good stability (+30 mV or more) at pH 5 or lower. For MCH-100 y MCH200 their biggest sizes are closer to their IEP at pH 11 and 10, respectively. For MCH-1000 now we appreciate that with more chitosan molecules their stability is on lower pHs and its size decreases as the pH is closer to the IEP.

All the above can be explained due to the fact that CH has higher ionization energy at lower pH values which helps to the biopolymer to have a less stable dispersion (close aggregation)[21] since the NH_3^+ are completely protonated.[22] The above mentioned aggregation phenomena makes the magnetic particle increase its size at lower pHs for most of the MCHs (except for MCH-200S) in comparison of the naked MNP. On the opposite at higher pH values CH has more unprotonated NH_2 species which produce H-bonding and generating agglomeration (open aggregation)[21] on the MCHs at some higher pH values.

Fig. 1. a) DLS and b) Zeta potential of MNP (black line), MCH-100 (orange line), MCH-100S (purple line), MCH-200 (olive line), MCH-200S (Blue line) and MCH1000 (pink line).

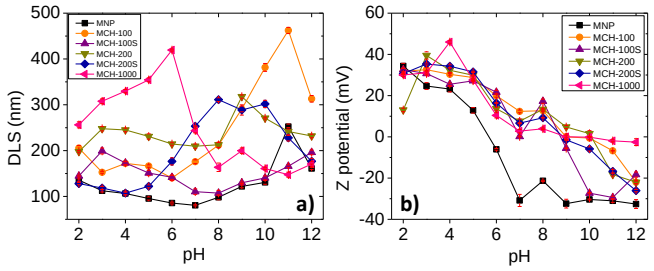

It is notable that small amounts of CH can modify the magnetite preserving their charge stabilities. In figure 2a and 2b we can make a closer comparison of MCH-100 and MCH-100S, where meanwhile their surface charges remain similar, for MCH-100 the charge drop is more gradual and staggered than in MCH-100S. Another significant difference is that MCH100S has less agglomeration presenting smaller sizes at pH 7 and 8, like the naked MNP, which can mean that in those pH values the effect of the CH on the particle is overlapped by the magnetite. Contrary to its counterpart MCH-100 possess broad range of sizes, this large size can allow the CH open-up and generate more activity points for metal ion absorption[1], which is highly beneficial for water treatment purposes. For the reasons mentioned above MCH-100 was chosen to perform water treatment analysis for the improvement of RW, so in the future this sample will be named just as MCH.

The characterization of MNP, and MCH are shown in Figure 3. Thermogravimetric analysis (TGA) was carry through to confirm the surface functionalization of the MNP with CH. The content of the surface-modified molecule was evaluated based on the weight loss ratio. As we can see in Figure 3a, the mass loss until 100 °C of MNP, CH, and MCH were 0.36%, 8.8 and 3.4%, respectively, which can be attributed to removal of the physically adsorbed water and/or hydroxyl groups on the surface of the materials.[23,24] For the MNP, another weight loss is observed in the range of 200-350 °C (~1.6%), related to the elimination of organic matter from both the solvents used and the secondary reaction products.[25] This total slight degradation by the effect of temperature indicates the good stability of the material. The thermogram for CH shows another step of degradation starting around 250 °C where this process involves the degradation of H_2O, NH_3, CO, CO_2 and CH_3COOH due the pyrolytic degradation of chitosan,[26] causing a weight loss of 81% in weight of the polymer at the end of the process. On the MCH thermogram, we found that the second part of the degradation process also starts close to 250 °C and there is a considerable weight loss of the material compared with the naked MNP which is caused by the pyrolytic degradation of chitosan part in the material. This degradation culminates in a total material weight loss of 30.37%, indicating an effective chemical modification of the MNP.

Fig. 2. Comparison of a) DLS and b) Zeta potential of MCH-100 (orange line) vs MCH-100S (purple line).

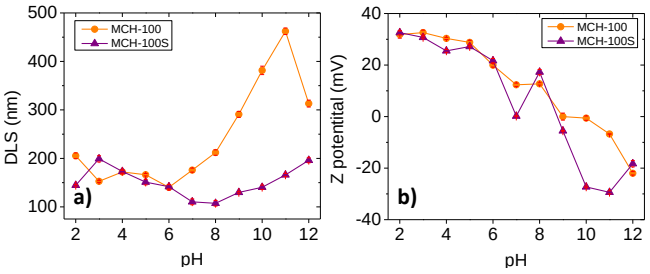

Naked MNP, CH and MCH were characterized by FT-IR spectroscopy (Figure 3b). The signal around 3400 cm^{-1} in MNP, CH and MCH is certainly due to the presence of hydroxyl groups (O-H) from water bonding on the surface of the materials. For the MNP the large and characteristic signal at 550 cm^{-1} is related to the stretching of Fe-O bonds in Fe_3O_4.[27] For CH, the first signal is also overlapped with the amide N-H signal, which presents a characteristic double peak, besides, at 1658 cm^{-1} the stretching vibration of the carbonyl from the amide I is located, accompanied by the bending signal of amide II (C-NH_2) at 1576 cm^{-1}. Finally, around 1060 cm^{-1} we locate the stretching signal of C-O.[28] The MCH spectrum shows both contributions of MNP and CH. At 1650 and 1055 cm^{-1} we find the stretching vibration of the carbonyl of amide I and the stretching signal of C-O, respectively, from CH, and at 550 cm^{-1} characteristic signal of Fe-O from the magnetite. These spectra indicate the correct synthesis of MCH.

To know the morphology of the MNP and MCH the analysis was approached by SEM and STEM images. Figure 3c belongs to the SEM image for MNP where we can appreciate the agglomeration effect and have an outline of its surface area, letting us to verify that authentic nanometric

particles were synthesized although the aggregation of the particles as result of Van der Waals forces among particles.[29] Additionally we can infer that the material is close to 20 nm in size, or less. Figure 3d displays the STEM image of MCH obtained after drying a drop of aqueous dispersed material, where the formation of clusters was observed, with sizes that varies from 20-60 nm. This cluster formation is related to the modification of the magnetite (as seen in TGA analysis) and stronger electrostatic and Van der Waals interactions between particles (Figure 3a). The size difference between DLS and SEM/STEM measurements is attributed to wet and dried particles used in each case, where the hydrodynamic diameter of MNP and MCH, in colloidal suspension, is commonly greater than SEM/STEM due to adsorbed water molecules on the magnetite surface.[30]

Fig. 3. a) TGA b) FT-IR of: MNP (black line), CH (cyan line), and MCH (orange line). c) SEM image of MNP powder. d) STEM images of dried drop of aqueous dispersion of MCH.

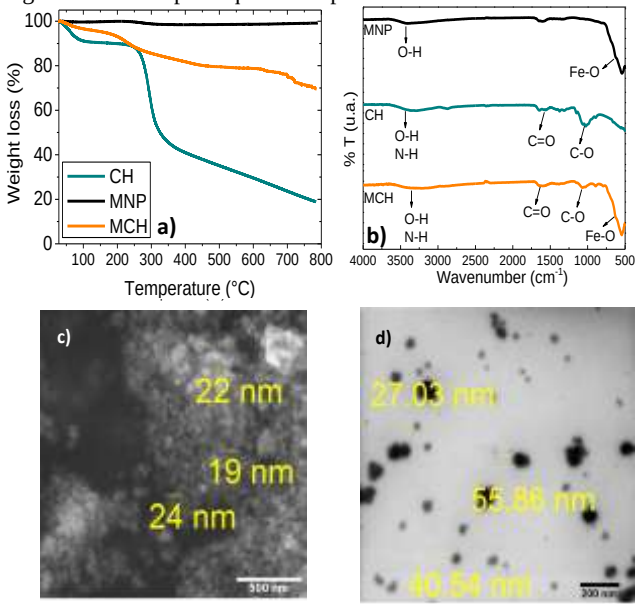

A BET analysis was performed to measure the surface area of magnetic materials indicating that MNP has a larger surface area (76.86 m^2g^{-1}) than MCH (72.70 m^2g^{-1}). These estimations allow to classify our magnetic materials as materials with moderated surface area compared with common active carbon that has around 500 m^2g^{-1}.

Model reclaimed water (RW) was obtained from a wastewater treatment plant in Tijuana, B. C. containing high levels of Ca^{2+} and Mg^{2+} as well as carbonates and other salts. Since natural pH of this water is 8, a pH range between 7 and 9 was studied to evaluate the electrostatic interaction of the magnetic materials for RW alkalinity and hardness removal. RW was treated with MNP and MCH in a dosage of 30 mg L^{-1}. After the treatment, the magnetic materials were recovered by magnetic decantation, and the recovered water was studied to measure the changes of their physicochemical parameters by DLS and Zeta potential.

Figure 4a and Figure 4b show the comparison between DLS and Zeta Potential for untreated RW and RW treated with the magnetic materials. RW treated with MCH has a considerable reduction on the particle sizes at each pH (Figure 4a), being more evident at pH 7 and 8 with sizes closer to 200 nm. MNP only show size reductions in some pH values, and in others, these particle sizes increased. The above is explained due to the change in its electric surface charges (Figure 4b). For water treated with MNP its Zeta potential was reduced to -4 mV, while for MCH switch its potential to more negative values (at pH 9), inducing the agglomeration of suspended particles. Besides, for MCH at pH 7 the electric surface charges are reduced adjacent to its IEP, while at pH 8 this value is reduced close to -3 mV. The van der Waals interactions between the superficial charge of the magnetic materials and the cations (as Ca^{2+} and Mg^{2+}), contained in the RW, are the responsible for all these changes on the particle surface charge and sizes.[31]

Fig. 4. a) DLS measurements and b) Comparison of the zeta potential measurements of untreated RW (green), and RW treated with MNP (black) and MCH (orange) at pH of 7, 8, and 9.

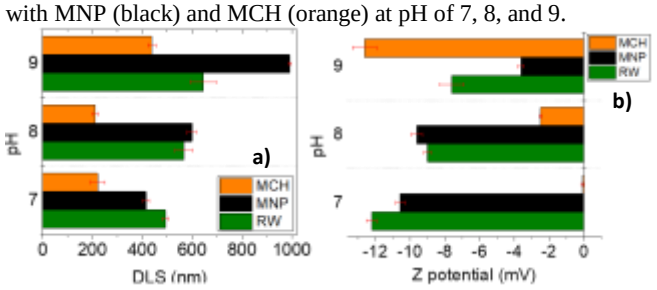

The parameters followed to evaluate the efectiveness of the magnetic products (MNP and MCH) to improve RW quality were alkalinity and hardness.

In Figure 5 we can examine the removal percentages obtained after treat RW with MNP and MCH (as mg L^{-1} of $CaCO_3$) where the maximum alkalinity removal (Fig. 5a) is achieved with treatment using MCH at pH 7 (23.5%), and pH 8 (22.3%). This results indicate an important reductton of this paremeter at the natural pH of the RW.

Fig. 5. a) Comparison of the alkalinity removal of MNP (black) and MCH (orange). b) Comparison of the hardness removal of MNP (black) and MCH (orange). At pH of 7, 8, and 9, expressed as percentage in mg L^{-1} of $CaCO^3$.

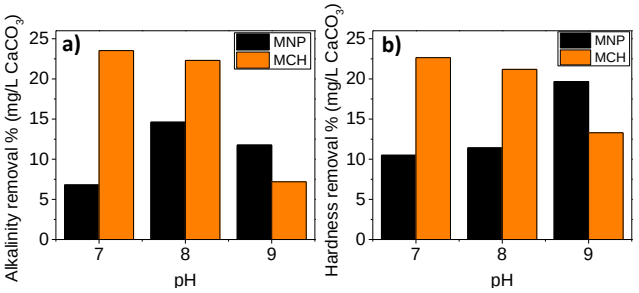

There are no maximum values established by the EPA or another institution for harness in reclaimed water, but there are some recomendations depending on the porpuse of its final destination, and it is necessary to reduce the hardness

of the waters to avoid scale formation and deposits in pipes and containers. As displayed Figure 5b, at pH 7 and pH 8 MCH achieved the maximun level of hardness removal by 22.4% and 21%, respectively.

Its importante to point that both magnetic materials accomplish the removal of a certain percentage of alkalinity and hardness, bringing those values closer to the requirement suggest by EPA and operations manuals.[32,33] These results (% of removal of alkalinity and hardness) give evidence of the functionality of CH in the magnetite to improve the quality of a RW.

3. CONCLUSIONS AND RECOMENDATIONS

Thanks to the chemical modification of magnetite, we developed magnetic chitosan (MCH) which it is been proved that act as a magnetic nano softener.

We found that MNP and MCH demonstrated to be effective for trapping and removing carbonates (as alkalinity and hardness) from real reclaimed water. Both magnetic materials show a potential application water conditioning. MCH proved to be effective for removing alkalinity and hardness with percentages greater than 20% at pHs 7 and 8.

At the same time, we have the possibility of recovering magnetic nanomaterials for further use and reduce the operation cost. This characteristic need to be tested in further investigations along with their capacity to remove other contaminants present in recovered water, not studied in this work.

Acknowledgments:
Authors would like to thank Consejo Nacional de Ciencia y Tecnología (CONACYT), Mexico for supporting the project APN2016-2015. Miss Estephany Santiago thanks CONACYT for the Ph.D. grant.

4. REFERENCES

[1] Liu, X.; Hu, Q.; Fang, Z.; Zhang, X.; Zhang, B. Magnetic Chitosan Nanocomposites: A Useful Recyclable Tool for Heavy Metal Ion Removal. *Langmuir* **2008**, *25* (1), 3–8.

[2] Bhateria, R.; Singh, R. A Review on Nanotechnological Application of Magnetic Iron Oxides for Heavy Metal Removal. *J Water Process Eng* **2019**, 30 (100845) 1-10.

[3] Xu, P.; Zeng, G. M.; Huang, D. L.; Feng, C. L.; Hu, S.; Zhao, M. H.; Lai, C.; Wei, Z.; Huang, C.; Xie, G. X.; et al. Use of Iron Oxide Nanomaterials in Wastewater Treatment: A Review. *Sci Total Envi* **2012**, 424, 1–10.

[4] Mohammed, L.; Gomaa, H. G.; Ragab, D.; Zhu, J. Magnetic Nanoparticles for Environmental and Biomedical Applications: A Review. *Particuology* **2017**, *30*, 1–14.

[5] Schwaminger, S. P.; Bauer, D.; Fraga-García, P.; Wagner, F. E.; Berensmeier, S. Oxidation of Magnetite Nanoparticles: Impact on Surface and Crystal Properties. *Cryst Eng Comm* **2017**, *19* (2), 246–255.

[6] Cîrcu, M.; Nan, A.; Borodi, G.; Liebscher, J.; Turcu, R. Refinement of Magnetite Nanoparticles by Coating with Organic Stabilizers. *Nanomaterials* **2016,** *6* (228), 1-12

[7] Silva, S. M.; Tavallaie, R.; Sandiford, L.; Tilley, R. D.; Gooding, J. J. Gold Coated Magnetic Nanoparticles: From Preparation to Surface Modification for Analytical and Biomedical Applications. *Chem Commun* **2016**, *52*, 7528-7540

[8] Pham, X.-H.; Hahm, E.; Kim, H.-M.; Son, B. S.; Jo, A.; An, J.; An, T.; Thi, T.; Nguyen, D. Q.; Jun, B.-H. Silica-Coated Magnetic Iron Oxide Nanoparticles Grafted onto Graphene Oxide for Protein Isolation. *Nanomaterials* **2020**, *10* (1), 117.

[9] Khasraghi, S. S.; Shojaei, A.; Sundararaj, U. Highly Biocompatible Multifunctional Hybrid Nanoparticles Based on Fe3O4 Decorated Nanodiamond with Superior Superparamagnetic Behaviors and Photoluminescent Properties. *Mater. Sci Eng C* **2020**, *114*, 110993.

[10] Satpathy, T. Chitosan Used In Pharmaceutical Formulations : A Review. *Pharm Rev* **2008**, *6* (3), 1-18.

[11] Singh, M. K.; Prajapati, S. K.; Mahor, A.; Rajput, N.; Singh, R. Chitosan: A Novel Exepient in Pharmaceutical Formulation. *Int J Pharm Sci Res* **2011**, *2*, 2266–2277.

[12] Aranaz, I.; Acosta, N.; Civera, C.; Elorza, B.; Mingo, J.; Castro, C.; De Los Llanos Gandía, M.; Caballero, A. H. Cosmetics and Cosmeceutical Applications of Chitin, Chitosan and Their Derivatives. *Polymers* **2018**, *10* (2), 213

[13] Zhao, D.; Yu, S.; Sun, B.; Gao, S.; Guo, S.; Zhao, K. Biomedical Applications of Chitosan and Its Derivative Nanoparticles. *Polymers* **2018**, *10* (4), 462.

[14] Periayah, M.; Halim, A.; Mat Saad, A. Biotechnology & Biomaterials Chitosan: A Promising Marine Polysaccharide for Biomedical Research. *Biotechno. Biomater* **2014**, *4* (4) 1000168.

[15] Manigandan, V.; Karthik, R.; Ramachandran, S.; Rajagopal, S. Chitosan Applications in Food Industry. *Biopolymers for Food Design* 2018, *20*, 469–491.

[16] Crini, N.; Lichtfouse, E.; Torri, G.; grégorio, C. Applications of Chitosan in Food, Pharmaceuticals, Medicine, Cosmetics, Agriculture, Textiles, Pulp and Paper, Biotechnology, and Environmental Chemistry. *Environ Chem Lett* **2019**, *17* (4), 1667-1692.

[17] Al-Manhel, A. J.; Al-Hilphy, A. R. S.; Niamah, A. K. Extraction of Chitosan, Characterisation and Its Use for Water Purification. *J Saudi Soc Agric Sci* **2018**, *17* (2), 186–190.

[18] Kangama, A.; Zeng, D.; Tian, X.; Fang, J. Application of Chitosan Composite Flocculant in Tap Water Treatment. *J Chem* **2018**, *2018* (2):1-9.

[19] Santiago, E.; Pina-Luis, G.; Martinez-Quiroz, M.; Perez-Landeros, O.; Rosas-González, N.; Valdez-Salas, B.; Oropeza-Guzman, M. T. Eco-Friendly Magnetic Nanoscavengers as Emerging Materials for Improving Reclaimed Water Quality. *Adv Sustain Syst* **2021**, *n/a* (n/a), 2000236.

[20] Liu, X.; Ma, Z.; Xing, J.; Liu, H. Preparation and Characterization of Amino–Silane Modified Superparamagnetic Silica Nanospheres. *J Magn Magn Mater* **2004**, *270* (1), 1–6.

[21] Roy, J.; Salaün, F.; Giraud, S.; Ferri, A.; Guan, J.; Chen, G. Solubility of Chitin: Solvents, Solution Behaviors and Their Related Mechanisms; *Sol poly* **2017**, *10*, 109-127

[22] Wang, Q. Z.; Chen, X. G.; Liu, N.; Wang, S. X.; Liu, C. S.; Meng, X. H.; Liu, C. G. Protonation Constants of Chitosan with Different Molecular Weight and Degree of Deacetylation. *Carbohydr Polym* **2006**, *65* (2), 194–201.

[23] Díaz-Hernández, A.; Gracida, J.; García-Almendárez, B. E.; Regalado, C.; Núñez, R.; Amaro-Reyes, A. Characterization of Magnetic Nanoparticles Coated with Chitosan: A Potential Approach for Enzyme Immobilization. *J Nanomater* **2018**, *2018*, 1-11.

[24] Karimzadeh, I.; Aghazadeh, M.; Doroudi, T.; Ganjali, M.; Kolivand, P. Superparamagnetic Iron Oxide (Fe3O4) Nanoparticles Coated with PEG/PEI for Biomedical Applications: A Facile and Scalable Preparation Route Based on the Cathodic Electrochemical Deposition (CED) Method. *Adv Phys Chem* **2017**, *2017* (1).

[25] Caamaño Chico, K. Síntesis, Caracterización y Funcionalización de Nanopartículas Magnéticas Para Detección de Patógenos. Estudio de La Funcionalización Con SiO2 Mesoporoso. Universidade da Coruña, **2016**.

[26] Corazzari, I.; Nisticò, R.; Turci, F.; Faga, M. G.; Franzoso, F.; Tabasso, S.; Magnacca, G. Advanced Physico-Chemical Characterization of Chitosan by Means of TGA Coupled on-Line with FTIR and GCMS: Thermal Degradation and Water Adsorption Capacity. *Polym Degrad Stab* **2015**, *112*, 1–9.

[27] Hussein-Al-Ali, S. H.; El Zowalaty, M. E.; Hussein, M. Z.; Geilich, B. M.; Webster, T. J. Synthesis, Characterization, and Antimicrobial Activity of an Ampicillin-Conjugated Magnetic Nanoantibiotic for Medical Applications. *Int J Nanomedicine* **2014**, *9*, 3801–3814.

[28] Dounighi, N.; Damavandi, M.; Zolfagharian, H.; Dehaghi, S. Preparing and Characterizing Chitosan Nanoparticles Containing Hemiscorpius Lepturus Scorpion Venom as an Antigen Delivery System. Archives of Razi Institute *67* (2), 145-153

[29] Ali, A.; Zafar, H.; Zia, M.; Ul Haq, I.; Phull, A. R.; Ali, J. S.; Hussain, A. Synthesis, Characterization, Applications, and Challenges of Iron Oxide Nanoparticles. *Nanotechnol Sci Appl* **2016**, *9*, 49–67.

[30] Sagar, V.; Atluri, V. S. R.; Tomitaka, A.; Shah, P.; Nagasetti, A.; Pilakka-Kanthikeel, S.; El-Hage, N.; McGoron, A.; Takemura, Y.; Nair, M. Coupling of Transient near Infrared Photonic with Magnetic Nanoparticle for Potential Dissipation-Free Biomedical Application in Brain. *Sci Rep* **2016**, *6* (1), 29792.

[31] Barakat, M. A. New Trends in Removing Heavy Metals from Industrial Wastewater. *Arab J Chem* **2011**, *4* (4), 361–377.

[32] U.S. Environmental Protection Agency, E. *Quality Criteria for Water*, 1st editio.; U.S. Environmental protection agency: Washington, D.C., 1976.

[33] U.S. Environmental Protection Agency, E. *2012 Guidelines for Water Reuse*; Washington, D.C., 2012.